

Response of Thermoacoustic Waves in Stressed Thin Plates

Shih-Ming Hsu, Ching-Chung Yin

Department of Mechanical Engineering
National Chiao Tung University
Hsinchu 300, Taiwan, Republic of China
E-mail: hsm89.me89g@nctu.edu.tw

Abstract- The response of thermoacoustic waves propagating in a thin plate exerted by mechanical stress is characterized by the phase velocity dispersion curves and attenuation spectra in this paper. The stressed thin plate is assumed to be insonified by an intensity modulated CW laser which is modeled as a Gaussian beam. The constitutive relations and governing equations are formulated within the framework of acoustoelasticity and thermo-elasticity. Attenuation spectra in the vicinity of folding frequency can be used as a significant index correlative to residual stress in the specimen. The amplitude and phase of thermoacoustic response are sensitive to the mechanical stress applied to specimen if loading direction is parallel to the direction of wave propagation.

Keywords- thermoacoustic reponse; residual stress; plate wave

I. INTRODUCTION

Determination of residual stresses in manufacturing is a major issue in the industries of semiconductor, flat panel display, steel, etc. In most studies, acoustoelasticity theory was used to determine residual stresses [1-2]. Thermoacoustic waves become rather important in recent years [3-5]. It has been shown that thermoacoustic wave has great potential in the application of residual stress measurement.

Laser-induced ultrasound and photoacoustics are thermal acoustic wave based nondestructive inspection techniques. Both have been received considerable attention in recent years because of either research interests or application purposes [6-9]. The former technique acquires the far-field response generated by pulsed laser, but the latter measures the near-field response resulted from intensity modulated CW laser. Laser-induced acoustic waves dissipate very fast in polycrystalline structures. The far-field response is too small to identify. It results in a need to understand the near-field, thermoacoustic wave response in the region close to the point-like thermal source.

When an intensity modulated beam of light is launched to a specimen, part of energy carried by the laser beam is reflected from the surface of the specimen. Part of it is converted to thermal energy and absorbed by the medium. The remaining energy transmits through the specimen if the medium is transparent or obscure. The temperature fluctuation results in a static dilatation and outgoing elastodynamic waves from the source.

This paper formulates the time-harmonic, thermoacoustic wave propagation within the framework of natural, initial, final coordinates provided by Pao *at al* [1]. It was originally used to establish the acoustoelasticity theory for determination of residual stresses in solids. The thermal waves possess inherent large attenuation which results in fast energy dissipation during propagation. Phase velocity dispersion curves and attenuation spectra for each mode of thermoacoustic waves in a thin copper plate under distinct stress states are determined numerically.

II. THEORETICAL FORMULATION

Refer to the Cartesian coordinate system (X_1, X_2, X_3) shown in Fig. 1 with the X_3 axis normal to plate surface such that the plate occupies the region $-\infty < X_1, X_2 < \infty, -h/2 < X_3 < h/2$. The incident laser beam is assumed to be modulated by a time-harmonic function such that its intensity becomes a steady-state output coupled with a harmonic fluctuation.

Let the width of the Gaussian profile be $2a$. The heat flux transmitted into the medium from Gaussian beam at the top surface, $X_3 = 0$, can be expressed by an amplitude modulation function in the form

$$q_3(X_1, X_2, 0, \omega) = Q_0 \exp[-(X_1^2 + X_2^2)/a^2] \\ = \frac{1}{4\pi^2} \int_{-\infty}^{\infty} \int_{-\infty}^{\infty} Q_3(k_1, k_2, 0, \omega) e^{i(k_1 X_1 + k_2 X_2)} dk_1 dk_2, \quad (1)$$

where $Q_3(k_1, k_2, 0, \omega)$ is the Fourier transform of the strength of incident beam at $X_3 = 0$ and

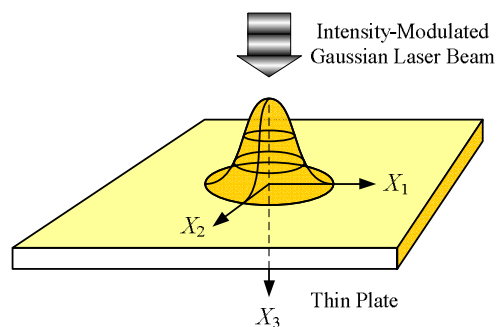


Figure 1. Schematic diagram of photoacoustic experiment.

$$Q_3(k_1, k_2, 0, \omega) = Q_0 \pi a^2 \exp[-(k_1^2 + k_2^2) a^2 / 4]. \quad (2)$$

The thermoacoustic response is represented as

$$u_3(X_1, X_2, X_3, \omega) = \frac{1}{4\pi^2} \int_{-\infty}^{\infty} \int_{-\infty}^{\infty} \frac{N(k_I, \omega)}{D(k_I, \omega)} Q_3 e^{i(k_1 X_1 + k_2 X_2)} dk_1 dk_2, \quad (3)$$

in which k_I ($I = 1, 2$) is wave number in the X_I direction. The zero denominator, $D(k_I, \omega) = 0$, yields the dispersion equation for thermoacoustic waves propagating in the thin plate.

A. Constitutive Relations

Consider a material body has undergone a deformation from natural state through initial state to final state as shown in Fig. 2. The natural state indicates the original state free of stress and strain. The initial state is a pre-deformed state in which residual stresses remain. When a thermal induced acoustic wave is superposed on the body in the initial state, the body is further deformed to the final state. Assume that there is no temperature change between the natural state and the initial state. The stress components T_{IJ} and the increment of entropy Ξ satisfy the following constitutive equations:

$$T_{IJ} = \bar{c}_{IJKL} u_{K,L} - \bar{\lambda}_{IJ} \Delta\Theta, \quad \Xi = \bar{\lambda}_{KLU_{K,L}} + \bar{\alpha} \Delta\Theta, \quad (4)$$

where the subscripts $I, J, K, L = 1, 2, 3$; $u_{K,L}$ and $\Delta\Theta$ indicates the strain changes and temperature rise caused by the external disturbance applied to the initial state. \bar{c}_{IJKL} , $\bar{\lambda}_{IJ}$ and $\bar{\alpha}$ denote the elastic constants, thermal modulus and thermal constant influenced by initial strains, respectively. They are of the form

$$\begin{aligned} \bar{c}_{IJKL} &= (1 - e_{NN}^i) c_{IJKL} + c_{IJKLMN} u_{M,N}^i + c_{OJKL} u_{I,O}^i \\ &\quad + c_{IOKL} u_{J,O}^i + c_{LOL} u_{K,O}^i + c_{IKO} u_{L,O}^i, \\ \bar{\lambda}_{IJ} &= (1 - e_{NN}^i) \lambda_{IJ} + \lambda_{OJ} u_{I,O}^i + \lambda_{IO} u_{J,O}^i, \\ \bar{\alpha} &= (1 - e_{NN}^i) \alpha, \end{aligned} \quad (5)$$

where $e_{NN}^i = u_{1,1}^i + u_{2,2}^i + u_{3,3}^i$ denotes cubic dilatation; c_{IJKL} , c_{IJKLMN} , λ_{IJ} and α are the second-order and third-order elastic constants, thermal modulus and thermal constant measured in the natural state, respectively. Both c_{IJKL} and c_{IJKLMN} possess symmetry property. The effective elastic constants involving residual stress effect are usually expressed in Voigt's notation. The correspondence between the initial strains $u_{K,L}^i$ and the initial (residual) stresses T_{IJ}^i is in the form of $T_{IJ}^i = c_{IJKL} u_{K,L}^i$.

B. Governing Equations

Based on the theory of acoustoelasticity, the elastic wave propagation in a medium under residual stress must satisfy the equations of motion in the initial state of the form

$$\frac{\partial}{\partial X_J} \left(T_{IJ} + T_{JK}^i \frac{\partial u_I}{\partial X_K} \right) = \rho_i \frac{\partial^2 u_I}{\partial t^2}, \quad (6)$$

where the mass density in the initial state is described by $\rho_i = (1 - e_{NN}^i) \rho_0$. Further, the balance of entropy and Fourier heat transfer equation in the initial state are of the form

$$\frac{\partial q_J}{\partial X_J} = -\Theta_i \frac{\partial \Xi}{\partial t}, \quad q_J = -\bar{k}_{JK} \frac{\partial (\Delta\Theta)}{\partial X_K}, \quad (7)$$

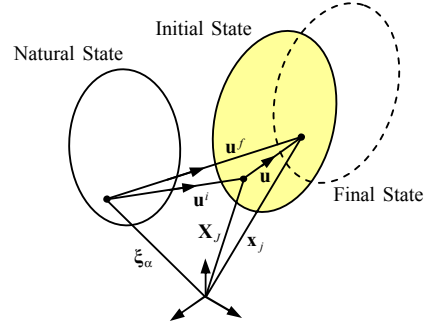


Figure 2. The coordinates at the natural, initial, and final states.

where Θ_i is the temperature in initial state, q_J the heat flux, \bar{k}_{JK} the thermal conductivity effected by the initial strains $u_{K,L}^i$. In the case of isotropic medium, they are in the form of

$$\begin{aligned} \bar{k}_1 &= (1 - e_{NN}^i) k + 2k u_{1,1}^i, \quad \bar{k}_2 = (1 - e_{NN}^i) k + 2k u_{2,2}^i, \\ \bar{k}_3 &= (1 - e_{NN}^i) k + 2k u_{3,3}^i, \quad \bar{k}_4 = \bar{k}_5 = \bar{k}_6 = 0. \end{aligned} \quad (8)$$

in which k is the thermal conductivity measured in the natural state.

Substitution of the constitutive equations (4) of a thermoelastic state with residual stress into (7) yields the differential equations of thermoelastic wave propagation as follows:

$$(\bar{c}_{IJKL} + T_{JL}^i \delta_{IK}) \frac{\partial^2 u_K}{\partial X_J \partial X_L} - \bar{\lambda}_{IJ} \frac{\partial (\Delta\Theta)}{\partial X_J} = \rho_i \frac{\partial^2 u_I}{\partial t^2}, \quad (9)$$

$$\left(\frac{\bar{k}_{JK}}{\Theta_i} \right) \frac{\partial^2 (\Delta\Theta)}{\partial X_J \partial X_K} - \bar{\lambda}_{KL} \frac{\partial^2 u_K}{\partial t \partial X_L} = \bar{\alpha} \frac{\partial (\Delta\Theta)}{\partial t}. \quad (10)$$

C. Dispersion of Thermoelastic Waves

Consider that the displacements and temperature of a thermoelastic wave possess time-harmonic dependence in the form:

$$\begin{cases} u_I(X_J, t) \\ \Delta\Theta(X_J, t) \end{cases} = \begin{cases} U_I(k_J, \omega) \\ U_4(k_J, \omega) \end{cases} \exp[i(k_J X_J - \omega t)]. \quad (11)$$

Substituting (11) back into (9)-(10) results in a thermoelastic Christoffel equation as follows:

$$\begin{bmatrix} k^2 \bar{\Gamma}_{IK} - \omega^2 \rho_i \delta_{IK} & ik \bar{\Lambda}_I \\ \omega k \bar{\Lambda}_K & \Theta_i^{-1} k^2 \bar{K} - i\omega \bar{\alpha} \end{bmatrix} \begin{Bmatrix} U_K \\ U_4 \end{Bmatrix} = 0 \quad (12)$$

where $\bar{\Gamma}_{IK} = n_J n_L (\bar{c}_{IJKL} + T_{JL}^i \delta_{IK})$, $\bar{\Lambda}_I = n_J \bar{\lambda}_{IJ}$, $\bar{K} = n_K \bar{k}_{JK}$. The non-trivial solution of (12) provides a characteristic equation, in which the phase velocity c along a prescribed propagating direction $\mathbf{n} = [n_1, n_2, n_3]$ are an implicit function of the angular frequency ω .

Consider a thin isotropic plate structure as an example. A thermoelastic wave is assumed to propagate along the X_1 -axis. Therefore (12) can be decomposed into an individual equation for SH wave as well as a set of coupled equations for P-SV waves and thermal wave. The coupled Christoffel equations for P-SV waves and thermal wave are given by

$$\begin{bmatrix} k^2 \bar{\Gamma}_{11} - \omega^2 \rho_i & k^2 \bar{\Gamma}_{13} & ik \bar{\Lambda}_1 \\ k^2 \bar{\Gamma}_{13} & k^2 \bar{\Gamma}_{33} - \omega^2 \rho_i & ik \bar{\Lambda}_3 \\ \omega k \bar{\Lambda}_1 & \omega k \bar{\Lambda}_3 & \Theta_i^{-1} k^2 \bar{K} - i\omega \bar{\alpha} \end{bmatrix} \begin{Bmatrix} U_1 \\ U_3 \\ U_4 \end{Bmatrix} = 0. \quad (13)$$

The products of wave number k and the components of wave normal n_1, n_3 in (13) will be replaced by k, ζ , respectively.

The characteristic equation is a cubic polynomial in terms of the square of wave number ζ^2 . It should be noted that the roots ζ_j may be real or complex and for definiteness we assume $\text{Im}(\zeta_j) \geq 0$ ($j = 1, 3, 4$). Let the eigenvalues be expressed as $\pm \zeta_1, \pm \zeta_2, \pm \zeta_3$, respectively. The term with $\text{Re}(\zeta) > 0$ corresponds to the down-going waves propagating along the positive X_3 direction. On the other hand, the term with $\text{Re}(\zeta) < 0$ denotes those up-going waves traveling toward the negative X_3 direction. The eigenvector components, $U_1^\pm, U_3^\pm, U_4^\pm$, are proportional to the parameters p_{ij}^\pm as follows:

$$\frac{U_1^{\pm(j)}}{p_{1j}^\pm} = \frac{U_3^{\pm(j)}}{p_{3j}^\pm} = \frac{U_4^{\pm(j)}}{p_{4j}^\pm} = C_j^\pm \quad (14)$$

where $p_{1j}^\pm, p_{3j}^\pm, p_{4j}^\pm$ denote the determinants of corresponding submatrices in (13).

The thermoelastic waves propagating in a thin plate are dispersive because of geometric constraints on the upper and the bottom boundaries. The surface traction and surface heat flux are assumed to be free on both boundary surfaces ($X_3 = \pm h$), i.e., $T_{13} = T_{33} = q_3 = 0$. The dispersion equations for symmetric and anti-symmetric modes are derived as follows:

$$D^{S,A}(k, \omega) = \det \begin{pmatrix} q_{11}^{S,A} & q_{13}^{S,A} & q_{14}^{S,A} \\ q_{31}^{S,A} & q_{33}^{S,A} & q_{34}^{S,A} \\ q_{41}^{S,A} & q_{43}^{S,A} & q_{44}^{S,A} \end{pmatrix} = 0 \quad (15)$$

with

$$\begin{aligned} q_{1j}^S &= \sin(k \zeta_j X_3) q_{1j}^+, & q_{1j}^A &= \cos(k \zeta_j X_3) q_{1j}^+, \\ q_{3j}^S &= \cos(k \zeta_j X_3) q_{3j}^+, & q_{3j}^A &= i \sin(k \zeta_j X_3) q_{3j}^+, \\ q_{4j}^S &= \sin(k \zeta_j X_3) q_{4j}^+, & q_{4j}^A &= \cos(k \zeta_j X_3) q_{4j}^+, \\ q_{1j}^+ &= i \zeta_j \bar{c}_{55} p_{1j}^+ + ik \bar{c}_{55} p_{3j}^+, & q_{4j}^- &= -i \zeta_j \bar{K}_3 p_{4j}^+, \\ q_{3j}^+ &= ik \bar{c}_{13} p_{1j}^+ + i \zeta_j \bar{c}_{33} p_{3j}^+ - \bar{\lambda}_3 p_{4j}^+. \end{aligned}$$

III. RESULTS AND DISCUSSION

The dispersion relation is a complex equation in terms of complex roots $k = \omega/c + i\eta$, in which the imaginary part is named the attenuation. A wave does not propagate far away if the attenuation η is large. The complex roots were determined through a numerical scheme using the simplex method to find the minimum magnitudes of the dispersion function.

Figs. 3-6 show the phase velocity dispersion curves and attenuation spectra for antisymmetric and symmetric modes of thermoacoustic waves propagating along the X_1 direction in a copper foil. With increase of frequency, the phase velocities of A_0 and S_0 modes converge to a constant speed corresponding to Rayleigh wave speed. The attenuations of both fundamental modes also merge together. The convergent value is about -12

dB/mm at 100 MHz. Four stress states, including initial state, biaxial stress state, and uniaxial stress states loaded in X_1 and X_2 directions, were considered. The physical constants for copper foil [10] used in numerical computation are listed below.

$$\begin{aligned} h &= 0.1 \text{ mm}, & \Theta_0 &= 300^\circ \text{ K}, & \rho_0 &= 8,920 \text{ kg/m}^3, \\ c_{11} &= 188.1 \text{ GPa}, & c_{111} &= -1,894 \text{ GPa}, & c_{144} &= -401 \text{ GPa}, \\ c_{12} &= 108.9 \text{ GPa}, & c_{112} &= -745 \text{ GPa}, & c_{155} &= -287 \text{ GPa}, \\ c_{44} &= 39.6 \text{ GPa}, & c_{123} &= 56 \text{ GPa}, & c_{456} &= 75 \text{ GPa}, \\ \gamma_3 &= 19 \times 10^{-6} / ^\circ \text{ K}, & \lambda_3 &= (3c_{12} + 2c_{44}) \gamma_3, \\ C_E &= 385 \text{ J/kg}^\circ \text{ K}, & k_3 &= 398 \text{ W/m}^\circ \text{ K}. \end{aligned}$$

The phase velocity variations caused by biaxial or uniaxial stress applied in the X_1 or X_2 direction are distinguishable in higher order modes. Except A_0 mode, the attenuation spectrum of each mode has its own minimum at a specific frequency, which is called the folding frequency. Thermoacoustic waves can propagate farther away at folding frequency because of smaller attenuation. The value is correlative to the magnitude of residual stress in the frequency range lower than folding frequency. Beyond the folding frequency, attenuation of each mode reaches to a large value, thereafter slowly decreases with increase of frequency. Mechanical tensile stress applied to the specimen in any direction increases the value of minimum attenuation for thermoacoustic waves traveling along the same direction. The effect diminishes in the transverse direction.

The amplitude of thermoacoustic response is dominated by the attenuation spectra. The differences among the attenuation spectra for distinct mechanical stress states are clear around the folding frequency. The amplitude measured in the vicinity of folding frequency can be used as an index for residual stress. Further, the phase velocity variation of S_0 mode is really distinguishable for different mechanical stress applied to the specimen as contrasted with A_0 mode. The S_0 mode is superior to other modes in determining residual stress using amplitude and phase of the response of thermoacoustic waves.

The computation of frequency response can be carried out by wave-number integration such as the modified Clenshaw-Curtis numerical scheme [11]. The transient response due to pulsed laser source are further determined from frequency responses through the inverse fast Fourier transform. Before executing lengthy computation, the attenuation spectra provide us the detailed characteristics of the thermoacoustic waves.

IV. CONCLUSION

The response of thermoacoustic waves propagating in a thin plate subjected to mechanical stress is characterized by the phase velocity dispersion curves and attenuation spectra. Except A_0 mode, the attenuation spectrum of each mode has a minimum at its own folding frequency. The attenuation spectra for distinct mechanical stress states have distinguishable changes in the vicinity of folding frequency. Amplitude change of thermoacoustic response corresponds to the magnitude of attenuation. Amplitude spectra around folding frequency can be used as an index correlative to residual stress. The S_0 mode has better potential than other modes in determining residual stress in low frequency range.

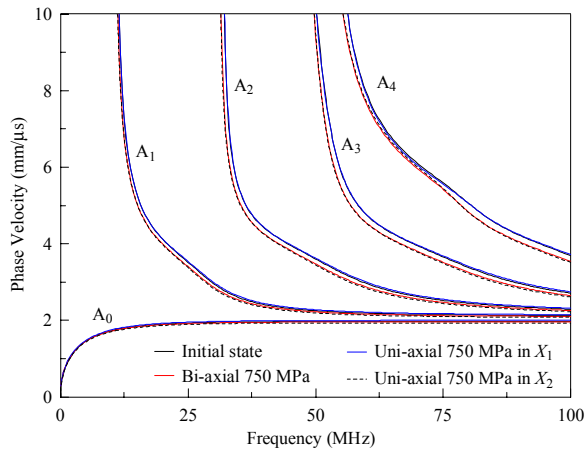


Figure 3. Phase velocity dispersion curves of antisymmetric modes.

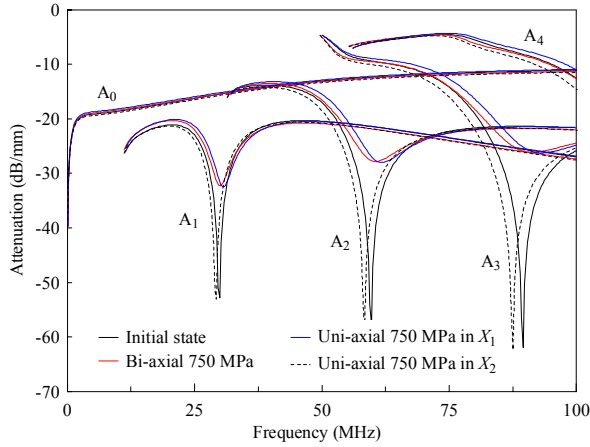


Figure 4. Attenuation spectra of antisymmetric modes.

A copper foil under four stress states, including initial state, biaxial stress state, and uniaxial stress states loaded in the X_1 and X_2 directions, were considered in numerical investigation. Computational results show that variations in amplitude and phase of thermoacoustic response are sensitive to mechanical stress applied to the specimen if loading direction is parallel to the direction of wave propagation.

ACKNOWLEDGMENT

The financial support of this work from National Science Council of the Republic of China through grant NSC 94-2212-E-009-003 is gratefully acknowledged.

REFERENCES

- [1] Y.-H. Pao, W. Sachse, and H. Fukuda, "Acousto-elasticity and ultrasonic measurements of residual stress," in *Physical Acoustic: Principles and Methods*, edited by W. P. Mason and R. N. Thurston (Academic Press, New York), Vol. 17, pp. 61-143, 1984.
- [2] A. V. Osetrov, H.-J. Fröhlich, R. Koch, and E. Chilla, "Acoustoelastic effect in anisotropic layered structures," *Phys. Rev. B*, Vol. 62, No. 21, pp. 13963-13969, 2000.
- [3] J. N. Sharma and H. Singh, "Generalized thermo-elastic waves in anisotropic media," *J. Acoust. Soc. Am.*, Vol. 85, No. 4, pp. 1407-1413, 1989.

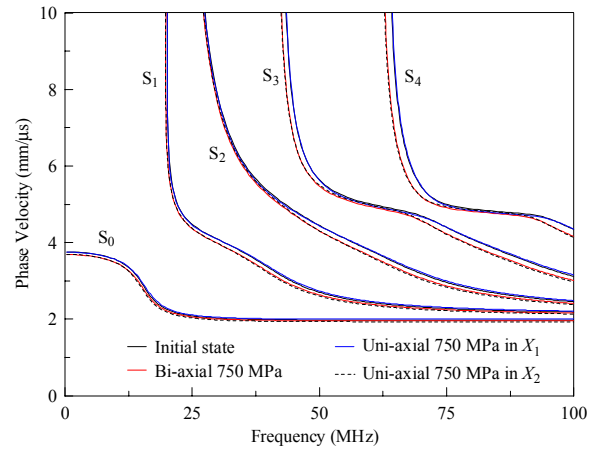


Figure 5. Phase velocity dispersion curves of symmetric modes.

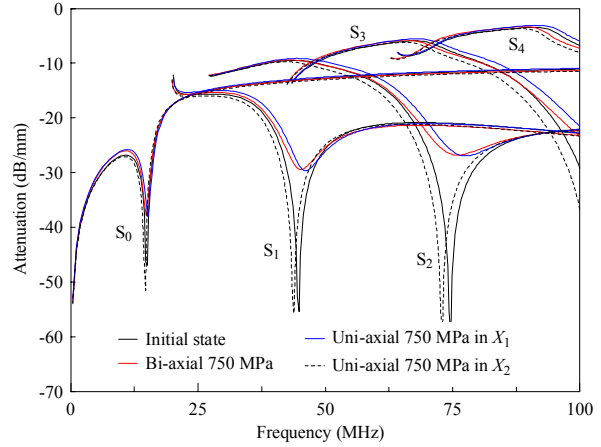


Figure 6. Attenuation spectra of symmetric modes.

- [4] J. N. Sharma, D. Singh, and R. Kumar, "Generalized thermoelastic waves in homogeneous isotropic plates," *J. Acoust. Soc. Am.*, Vol. 108, No. 2, pp. 848-851, 2000.
- [5] B. Singh, "Wave propagation in an anisotropic generalized thermoelastic solid," *Indian. J. Pure Appl. Math.*, Vol. 34, No. 10, pp. 1479-1485, 2003.
- [6] J. A. Rogers and K. A. Nelson, "Photoacoustic determination of the residual stress and transverse isotropic elastic moduli in thin films of the polyimide PMDA/ODA," *IEEE Trans. Ultras. Ferr. Freq. Contr.*, Vol. 42, No. 4, pp. 555-566, 1995.
- [7] J.-C. Cheng and Y. H. Berthelot, "Theory of laser-generated transient Lamb waves in orthotropic plates," *J. Phys. D: Appl. Phys.*, Vol. 29, pp. 1857-1867, 1996.
- [8] J.-C. Cheng, T.-H. Wang, and S.-Y. Zhang, "Normal mode expansion method for laser-generated ultrasonic Lamb waves in orthotropic thin plates," *Appl. Phys. B*, Vol. 70, pp. 57-63, 2000.
- [9] H. M. Al-Qahtani, S. K. Datta, and O. M. Mukdadi, "Laser-generated thermoelastic waves in an anisotropic infinite plate: FEM analysis," *J. Thermal Stresses*, Vol. 28, pp. 1099-1122, 2005.
- [10] S. Ballandras, E. Gavignet, E. Bigler, and E. Henry, "Temperature derivatives of the fundamental elastic constants of isotropic materials," *Appl. Phys. Lett.*, Vol. 71, No. 12, pp. 1625-1627, 1997.
- [11] S. Lih and A. K. Mal, "Elastodynamic response of a unidirectional composite laminate to concentrated surface loads, Part II," *ASME J. Appl. Mech.*, Vol. 59, pp. 887-892, 1992.